Original Research Article

KINETIC, EQUILIBRIUM AND THERMODYNAMIC STUDY OF GROUNDNUT OIL BLEACHING USING ACTIAVTED RICE HUSK AS ADSORBENT

ABSTRACT

Kinetic, equilibrium and thermodynamic studies of the bleaching of crude groundnut oil at optimized conditions was carried out using activated rice husk as an adsorbent for the bleaching process. Efficiency of bleaching was estimated by measuring the absorbance using a double-beam spectrophotometer at a wavelength of 450nm. The effects of adsorbent dosage, bleaching temperature and contact time on the bleaching efficiency were studied. A directly proportional relationship was found between dosage and contact time and the bleaching efficiency while a bell curve was discovered for temperature increase. The surface area of the rice husk increased from 150.32 to 1450.32 m^2/g while the pore volume decreased from 0.15524 to 0.12844 cm^3/g after activation which was determined via a Brunauer-Emmet-Teller (BET) analysis and the results further validated by the Scanning Electron Microscopy (SEM) images obtained. The kinetic data of the bleaching process were best described by the pseudo-second order kinetic model while the equilibrium adsorption isotherm analysis showed that the results from the Temkin isotherm were the most significant. The thermodynamic study revealed that the adsorptive bleaching process is feasible, spontaneous and exothermic with a decrease in entropy. The enthalpy value also showed that the adsorption process is predominantly physisorption. This study has revealed that an effective adsorbent can be produced from rice husk under optimized process conditions.

Keywords: Kinetic Models, Temkin Isotherm, Thermodynamic Parameters, Adsorption.

1.INTRODUCTION

A vegetable oil made from peanut seed that is taxonomically categorized as *Arachis hypogaea* is known as groundnut oil, also known as Peanut oil or Arachis oil. This legume crop is mostly farmed for its palatable seeds.Commercially, there are three ways to extract peanut oil: hydraulic pressing, expeller, and solvent extraction. For almost complete oil recovery when hydraulic pressing is utilized, hot solvent extraction is then performed. Oil extraction with an expeller depends on internal pressure and friction that heats the meal and makes it easier to extract the oil. The amount of peanut oil removed with this procedure is about 50%. Hexane is used to extract the leftover oil, and it is then eliminated via an evaporation-condensation process. Utilization of petroleum hydrocarbons or other solvents is a need for solvent extraction. With hexane, 95% ethanol, or 100% ethanol, this procedure performs more well [1][2].

One of the byproducts of rice processing in the rice mills is rice husk. When paddy rice is husked in the first step of milling, the husk is created, and it is later stripped from other components of the rice grain. As a waste-utilization resource that adds value and lowers processing costs in both home and commercial settings, rice husks have gained popularity as a resource. As a by-product

of rice milling, rice husk is commonly accessible in rice-producing nations like China and India, which produce 33% and 22% of the world's rice, respectively. Between 16 and 25 percent of paddy is made up of rice husks[3][4][5].Around 500 million tons of paddy are produced worldwide each year, yielding 120 million tons of rice husk annually. [6]. When rice husk is burned in an ambient environment, a byproduct is produced called rice husk ash. The globe produces 20 million tons annually [7][5]. Rice husks are not being used properly since people are unaware of their qualities and uses. As a result, the use of rice husk and rice husk ash in home and industrial processing not only helps to directly and indirectly increase farm revenue, but it also offers an alternate solution to the problem of how to dispose of rice husk.

Adsorption isotherms make predictions about the quantity of an adsorbate that would be absorbed by the surface of the adsorbent under typical time, temperature, and adsorbent use circumstances. The equilibrium between the refined oil adsorbate molecules and the surface of the rice husk will be demonstrated in this study. Among other equations, the Freundlich and Langmuir isotherms are employed to characterize the adsorption isotherms. These adsorption isotherms distinguish the adsorption process according to the kind of molecular interaction and describe the sorption activity of the majority of adsorbent.The adsorption rate may be calculated by fitting experimental data into several kinetic models, predicting how adsorbent and adsorbate will interact, and simulating the process. Pseudo-first order or pseudo-second order kinetics, among others, are good predictors of the rate kinetics for the adsorption process of bleaching groundnut oil.

This study aims to clarify the mode and extent of adsorption data using the Langmuir, Freundlich, Temkin, and Dubinin-Radushlkevich isotherms, as well as thermodynamic parameters (change in energy, enthalpy, and entropy), in order to better understand the bleaching mechanism of groundnut oil with a low-cost adsorbent (acid-activated rice husk).

2. MATERIALS AND METHODS

2.1 MATERIALS

Rice husk obtained from Gidan Kwanu village, Bida LGA Niger state was used to prepare the adsorbent. The groundnut oil was purchased from Jemaa LGA, Kaduna state. All the chemical used during the experiments were of analytical grade. The samples (adsorbent and oil) were prepared. This included the acid activation of the rice husk and the degumming and neutralization of the groundnut oil. The oil was optimally bleached according to an RSM CCD design with oil absorbance used as the response factor to check bleaching efficiency. The optimal process parameters were obtained and the kinetic, equilibrium and thermodynamic study were done at those conditions. The prepared adsorbent was characterized via BET and SEM analysis as well.

2.2 METHODS

2.2.1 BRUNAUER-EMMET-TELLER (BET) ANALYSIS

The equipment used for the analysis was the Nitrogen BET surface area and pore size analyzer (JW-DA). To determine the surface area of the rice husksample, the BET equation shown below was used:

$$\frac{1}{W\left[\left(\frac{P_O}{P}\right)-1\right]} = \frac{1}{W_M C} + \frac{C-1}{W_M C}\left[\frac{P}{P_O}\right] \quad (1)$$

Where W is the weight of nitrogen gas adsorbed at a relative pressure, P/P_0, W_M is the weight of adsorbate making up a monolayer of surface coverage, and C is the BET C constant. C is related to the energy of adsorption in the first adsorbed layer, so its value shows how strong the interactions between the adsorbent and the adsorbate are. The BET equation needs a linear plot of $1/[W(P_0/P)-1]$ vs. P/P_0. which, when nitrogen is used as the adsorbate, is limited to a lower limited area of the adsorption isotherm, usually in the P/P_0 range of 0.05 to 0.35, because the rice husk sample is microporous.

2.2.1.1 PREPARATIONS FOR SAMPLE ANALYSIS

The cold trap Dewar is filled with liquid Nitrogen to ¾ of its volume and is then mounted on the Autosorb-1. The He and N_2 cylinder valves as well as the ball valves which are located after the pressure regulators are opened and the cylinder pressure regulators are set to 10 psi.

2.2.1.2 DEGASSING SAMPLES PRIOR TO ANALYSIS

The right size cell with a fill glass rod (9 mm) was picked for the rice husk sample. The empty sample cell with the full glass rod was weighed and written down on a 5-place analytical scale. The fill glass rod was taken out of the cell, and the rice husk sample was put in using a tube until it filled up half of the cell. The fill glass rod sample was then put back into the cell. The sample cell, glass stick, and sample were all put on a scale. The weight of the sample was found by taking the original weight away from the weight of the sample before it was degassed. The cell was then put into a heating mantle and clamped into place. The cell and heating mantle were then connected to the sample preparation machine. The knurled retainer ring, plunger with O-ring, and cell adapter were all taken off the sample processing station and put on the sample cell. Then, the cell was put into the hole in the station, and the nut was lightly tightened. The temperature was set by hand to 200 °C, and the heat was turned on by moving the toggling switch to the "up" position. When degassing started, the green light started blinking. Because of how the sample was set up, degassing took 2 hours.

Figure 1: BET Surface Area Analyzer Model No JW-DA: 76502057en

2.2.2 SCANNING ELECTRON MICROSCOPY (SEM) ANALYSIS

Scanning Electron Microscope Model JOEL-JSM 76000F was the tool used to do the research. The rice husk samples were made by cutting them down to the right size so they would fit in the specimen chamber. They were then firmly attached to the specimen holder (also called a specimen stub). The samples were then covered with a layer of electrically conductive platinum, which was put on the rice husk by evaporating the platinum in a high pressure. The SEM device put the sample in a relatively high-pressure room with a short working distance and a differentially pumped electron optical column to keep the vacuum at the electron gun at a good level. In the ESEM, a high-pressure area around the sample cancels out the charge and boosts the secondary electron signal. This makes the picture of the rice husk sample better at higher magnifications. The low-voltage SEM study was done in a FEG-SEM because the field emission guns (FEG) can produce high primary electron brightness and a small spot size on the rice husk even at low acceleration potentials.

Figure 2: Scanning Electron Microscope Model JOEL-JSM 76000F

2.2.3 KINETIC, EQUILIBRIUM AND THERMODYNAMICEXPERIMENTS

To study the adsorption kinetics of activated carbon from rice husk, 30 ml of unbleached Groundnut oil was discharged into the bleaching vessel and bleached at the optimized variables obtained from the RSM. Samples were withdrawn and filtered for storage in sample containers for absorbance analysis.

The procedure was repeated for samples to be withdrawn after subsequent time intervals of 10 mins for the kinetic study, 1.5 g for the equilibrium studies at four different temperatures and 20 ℃ for the thermodynamic study.

2.2.3.1 ADSORPTION KINETICS

2.2.3.1.1 PSEUDO-FIRST-ORDER RATE EQUATION

The pseudo-first-order equation can be expressed in a non-linear equation as shown below

$$q_t = q_e[1 - exp(-k_1 t)] (2)$$

Where,q_t and q_e are adsorption capacity at time t and at equilibrium e, respectively, i.e., the amount of adsorbate per unit of adsorbent and k_1 is the pseudo-first-order constant t^{-1}.

2.2.3.1.2 PSEUDO-SECOND-ORDER RATE EQUATION

The pseudo-second-order equation can be expressed in a non-linear equation as shown below

$$q_t = \frac{q_e^2 k_2 t}{1 + q_e^2 k_2 t} (3)$$

Where k_2 is the pseudo-second-order constant t^{-1}.

2.2.3.1.3 INTRA-PARTICLE DIFFUSION

The Weber-Morris intra-particle diffusion model is expressed as

$$q_t = k_{id} t^{0.5} + C_i (4)$$

Where,k_{id} (mg/kg $min^{0.5}$) is the intra-particle diffusion rate constant and C_i (mg/kg) is associated to boundary layer thickness.

If intra-particle diffusion is the limiting step of the adsorption process, the plot q_t against $t^{0.5}$ is a straight line. Moreover, if this plot goes through the origin, intra-particle diffusion is the only rate-limiting step; if the plot presents two or more intercepting straight lines, adsorption involves independent steps.

2.2.3.1.4ELOVICH MODEL

The Elovich model can be expressed as shown below

$$q_t = \frac{1}{a} + \ln(1 + abt) (5)$$

Where, a is the parameter of the Elovich model associated with the initial velocity ($mgkg^{-1}min^{-1}$)

b is the desorption constant ($mgkg^{-1}$).

2.2.3.2 EQUILIBRIUM STUDIES

The isotherm parameters correlate the kinetics and thermodynamics of the adsorption process, providing a quantitative and qualitative estimation of the efficiency of the adsorbent. In this work, four adsorption isotherms were used to evaluate the optimum bleaching by adsorption of groundnut oil using activated rice husk as an adsorbent.

2.2.3.2.1 LANGMUIR ISOTHERM MODEL

The Langmuir model was the first model presenting a coherent theory of adsorption. It assumes a monolayer surface coverage, an independent and homogenous adsorbent surface, mostly applied to chemisorption. It is generally expressed in a non-linear model as shown below

$$q_e = \frac{q_{max} K_S C_e}{1 + K_S C_e} (6)$$

Where, q_e (mg/kg) is the amount of adsorbate per unit mass of adsorbent, C_e (mg/kg) is the equilibrium concentration of adsorbate in solution and q_{max} (mg/kg) and K_S $(mg/kg)^{-1}$ are Langmuir constants related to the adsorption capacity and rate of adsorption for the monolayer, respectively

2.2.3.2.2 FREUNDLICH ISOTHERM MODEL

The Freundlich model is an empirical one, assuming a heterogenous surface energy, i.e., stronger binding sites are occupied first and the binding strength decreases with an increasing degree of site occupation and it is not restrictive to monolayer coverage. It is generally described in its non-linear form as shown below

$$q_e = K_F C_e^n (7)$$

Where, K_F [(mg/kg) $(mg/kg)^{-n}$] is defined as the adsorption capacity of the adsorbent.

2.2.3.2.3TEMKIN ISOTHERM MODEL

A linear form of the Temkin Isotherm expression:

$$q_e = \frac{RT}{b_T} \ln A_T + \frac{RT}{b_T} \ln C_e (8)$$

Where A_T is the Temkin isotherm equilibrium binding constant $(L.mol^{-1})$,b_T is the Temkin isotherm constant (J/mol), R is the Universal Gas Constant $(J.mol^{-1}.K^{-1})$ and T is the absolute temperature (K)

2.2.3.2.4 DUBININ-RADUSHLKEVICH ISOTHERM MODEL

A linear form of the Dubinin-Radushkevich Isotherm expression:

$$\ln q_e = \ln q_D - 2B_D RT \ln(1 + 1/C_e) \quad (9)$$

$$E_D = \sqrt{1/2B_D} \quad (10)$$

Where B_D relates to the free energy of adsorption per mole of coloured oil pigment in the solution as it moves to the surface of the adsorbent from an infinite distance $(mol^2.kJ^2)$, q_D is the Dubinin–Radushkevich isotherm constant, which relates to the degree of sorbate sorption on the sorbent surface $(mg.g^{-1})$, E_D is the apparent energy of adsorption $(kJ.mol^{-2})$.

2.2.3.3 THERMODYNAMICS PARAMETERS

The Standard Gibbs Free Energy can provide the degree of exoergicity and the higher its absolute value reflects more energetically favourable adsorption. Whereas, enthalpy is important

to determine whether the adsorption process in chemical or physical, as it is shown in Equation 11

$$\Delta G^0_{ads} = -RT \ln(K_0) \quad (11)$$

Where, ΔG^0_{ads} (J/mol) is the standard Gibbs Free Energy, R is the universal gas constant (8.3145 $J \cdot mol^{-1} \cdot K^{-1}$), T (K) is the temperature and K_0 is the equilibrium constant (or the solute coefficient of distribution between the solid and liquid phases at equilibrium) which changes with temperature.

Standard Gibbs Free Energy might be expressed in terms of standard enthalpy (ΔH^0_{ads}) and standard entropy (ΔS^0_{ads}) according to Van't Hoff equation (12)

$$\ln(K_0) = -\frac{\Delta G^0_{ads}}{RT} = \frac{\Delta S^0_{ads}}{R} - \frac{\Delta H^0_{ads}}{RT} \quad (12)$$

3. RESULTS AND DISCUSSION

3.1 SCANNING ELECTRON MICROSCOPY (SEM) ANALYSIS OF THE ADSORBENT

Presented in thefigures below are the scanning electron micrographs of raw rice husk and the activated rice husk at various magnifications. The SEM images were studied for the surface and morphological characteristics in the adsorbent materials. In comparison with the raw rice husk, the SEM images showed clear changes in the micrographs of all the activated rice husk. This change in the SEM images revealed the structural changes in the modified adsorbent materials.

The images indicated uneven surfaces and non-uniform structures in both samples. The micrographs of the raw rice husk show structures that are few, relatively large with some smaller agglomerates situated on their surface and the structures situated in a porous matrix space with large interstitial pore spaces. This in agreement with the textural characterization obtained via BET analysis that showed the micro pore volume of the raw rice husk being greater than the activated rice husk. The micrographs of the activated rice husk show smaller, more numerous structures that are smoother, flatter without the random dispersion of agglomerates on their surface and well distributed in their matrix creating a much larger surface area which is further confirmed by the BET analysis that shows an 864.82% increase in surface area of the activated rice husk. The structures are also mildly more uniform tending to "filamentous" and "flake-like" shape that is both thin and elongated, with a branching or thread-like appearance that is also somewhat flat and irregular in shape.Changes in adsorption effectiveness between the two materials may be explained by morphological variations between the particles making them up; for instance, the adsorbent that was subjected to acid treatment displays a higher surface area of contact.

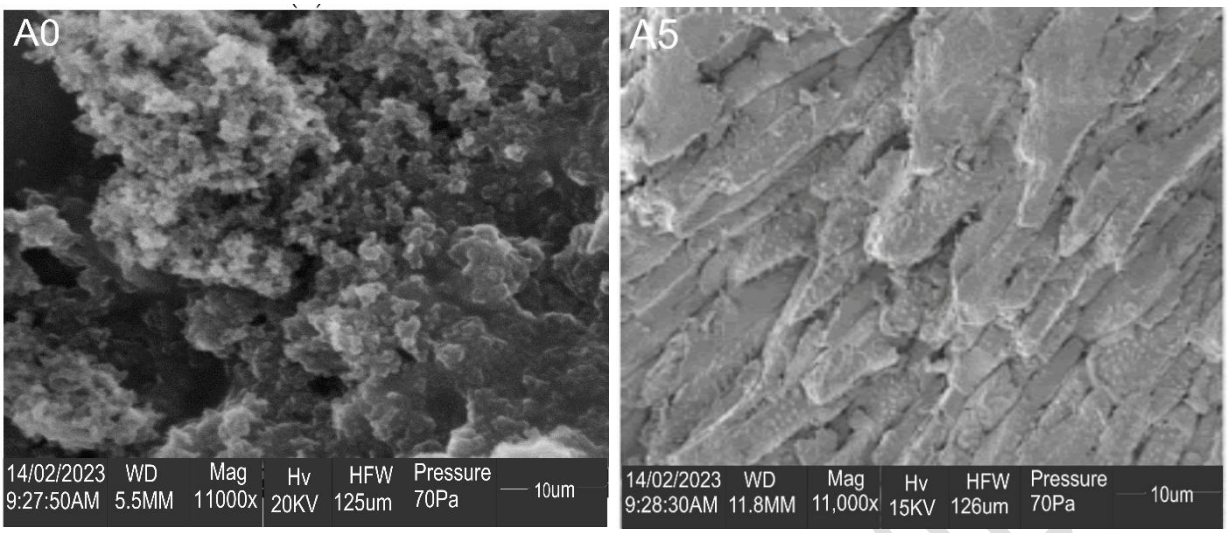

(a) (b)

Figure 3: Scanning electron micrographs of raw (a) and 3M H_2SO_4 activated (b) rice husk at 11000x magnification

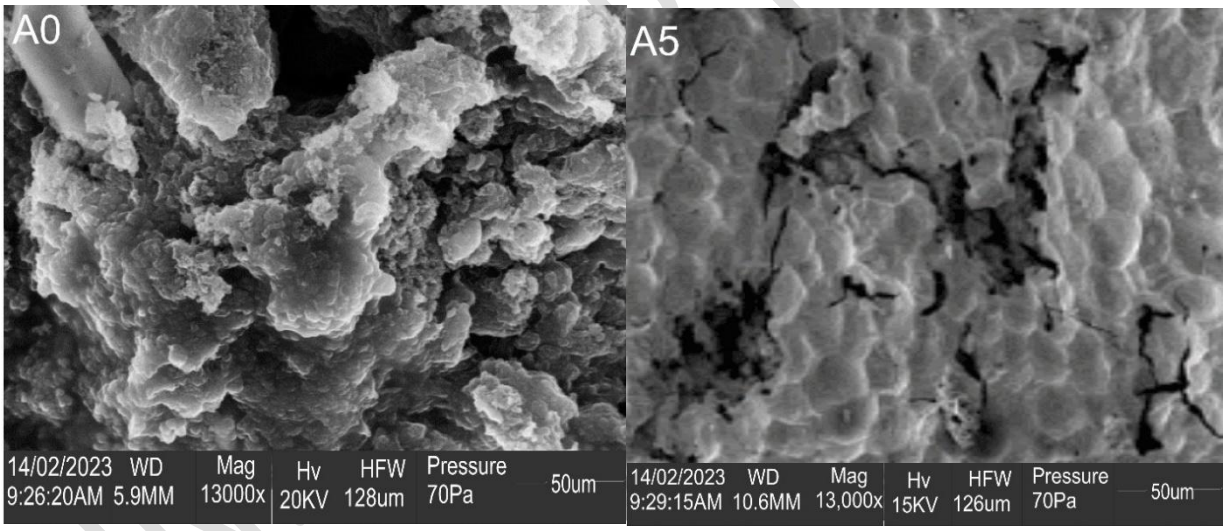

(a) (b)

Figure 4: Scanning electron micrographs of raw (a) and 3M H_2SO_4 activated (b) rice husk at 13000x magnification

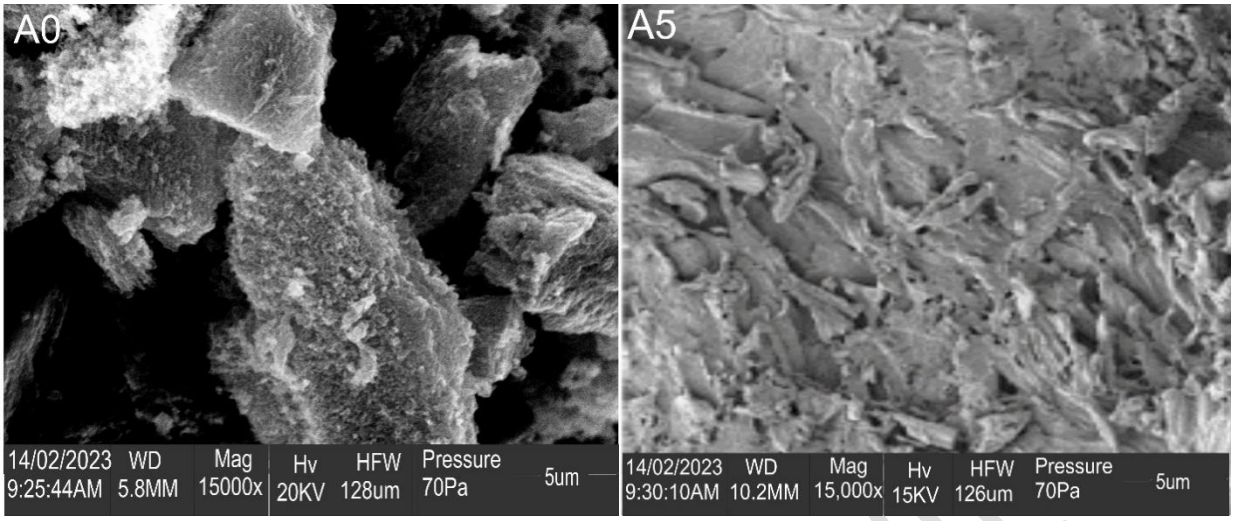

(a) (b)

Figure 5: Scanning electron micrographs of raw (a) and 3M H_2SO_4 activated (b) rice husk at 15000x magnification

3.2 BRUNAUER-EMMETT-TELLER ANALYSIS

Table 1 summarizes the BET characterization of the adsorbents (crude and activated) used in the bleaching procedure. It can be seen that the activated rice husk has a much larger surface area than that of the raw rice husk with a percentage increase of 864.82%. As reported by [9], the BET surface area of raw rice husk was found to be 320 m^2/g and this increase in surface area may be as a result of acid activation. The BET surface area of 1450.32 m^2/g achieved also matches works done by [10][11] and [12] whom prepared adsorbents from coconut shell, palm kernel shell and rice husk and achieved a BET total surface area of 2,451, 1,135 and 2,696 m^2/g respectively.

Micro pore volume and average pore width were both greater in raw rice husk than in activated husk. The scanning electron micrographs (SEM) of these two adsorbents corroborate this. It's possible that a greater quantity of oil will be impregnated at the conclusion of the adsorptive process if the pore spaces and volume are bigger, since this facilitates oil entry and increases access of the adsorbate to the adsorption sites inside the pore cavities[13]. The linear and log isotherms of the BET analysis for the crude and activated rice husk are presented in the figures below.

Table 1: Summary of the BET analysis of the crude and activated rice husk

Parameter	Crude Rice Husk	Activated Rice Husk
BET Total Surface Area (m^2/g)	150.32	1450.32

t-Plot Micro-pore Area (m^2/g)	50.12	50.23
Pore Volume of pores less than 1550.529 Å width (cm^3/g)	0.5545	0.6035
Pore Volume of pores less than 1226.916 Å width (cm^3/g)	0.60734	0.60548
t-Plot Micropore volume (cm^3/g)	0.15524	0.12844
BJH Desorption cumulative volume of pores	0.45222	0.52222
BET Adsorption average pore width (4V/A) (Å)	28.25	24.54
BET Desorption average pore width (4V/A) (Å)	28.22	24.42
BJH Adsorption average pore width (4V/A) (Å)	28.55	24.26
BJH Desorption average pore width (4V/A) (Å)	30.55	24.22

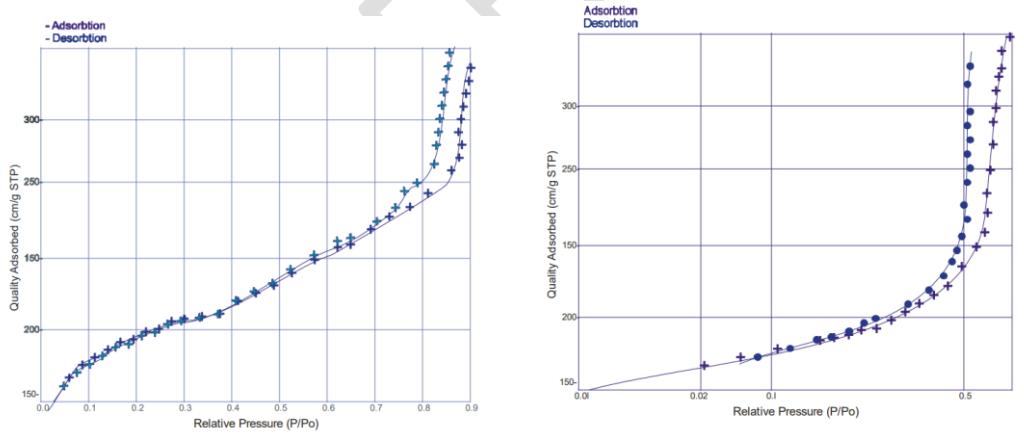

(a) (b)

Figure 6: Nitrogen adsorption BET linear (a) and log (b) isotherm plot of activated rice husk

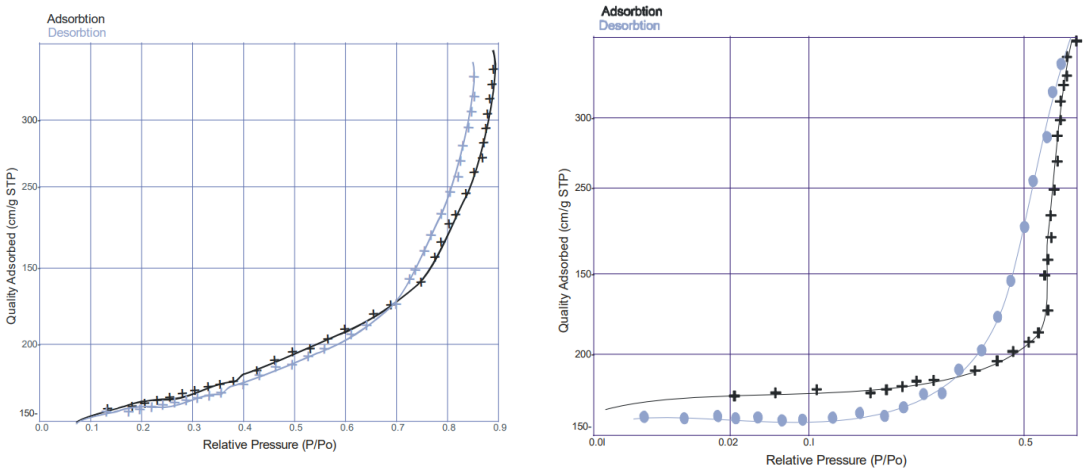

(a) (b)

Figure 7: Nitrogen adsorption BET linear (a) and log (b) isotherm plot of raw rice husk

Figures 8 shows the plots of the BJH adsorption cumulative pore volume for the raw and activated rice husk. The aggregate pore volume of a solid substance is shown graphically as a function of pore diameter in a plot known as the BJH (Barrett-Joyner-Halenda) plot. Adsorption isotherm data for the material are commonly acquired at cryogenic temperatures by gas adsorption methods like nitrogen adsorption, and the plot is created by fitting the BJH theory to this data. A porous material's pore size distribution may be determined via its adsorption isotherm values using the BJH theory. It assumes that the pores in the substances are cylindrical or slit-like and that the adsorbed gas atoms create a monolayer on the outermost layer of the substance.

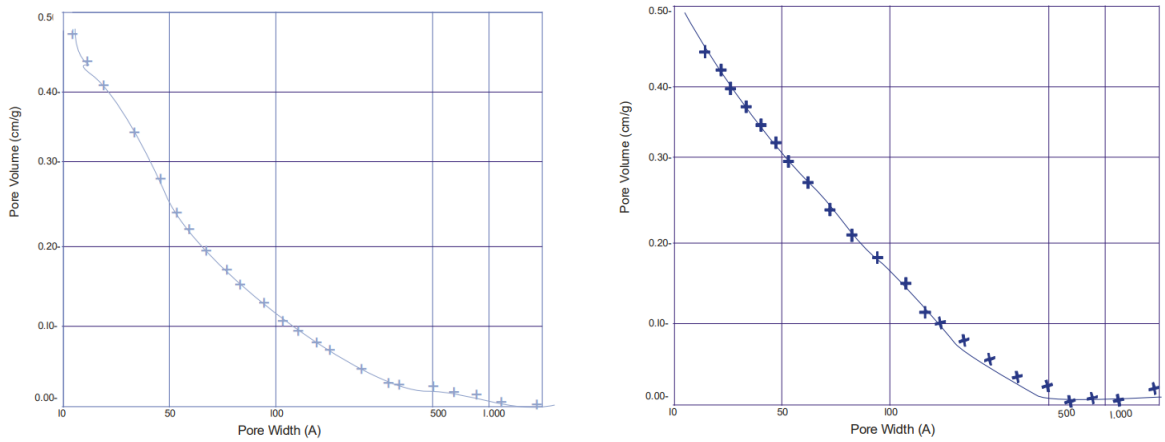

(a) (b)

Figure 8: BJH adsorption pore volume plot for the raw (a) and activated rice husk (b)

3.3 ADSORPTION CHARACTERISTICS OF THE BLEACHING PROCESS

3.3.1 EFFECT OF ADSORBENT DOSAGE ON THE BLEACHING PROCESS

Table 2: Absorbance and bleaching efficiency at varying adsorbent dosage

Dosage (g)	Absorbance (A450)	Bleaching Efficiency (%)
2.67	0.631	34.41
4.17	0.558	41.20
5.67	0.512	46.78
7.17	0.493	48.75
8.67	0.471	51.04

To study this effect, adsorption was performed at different adsorbent dosage within the range of 3.67-8.67g at constant optimum temperature, time and particle size (54 ℃, 22 min and 0.2 mm respectively). The crude groundnut oil has an absorbance of 0.962. As may be seen in Figure 4.27, the bleaching percentage rose as the adsorbent dose increased. It can be deduced that the adsorbent dose has an immediate impact on the bleaching process, with more adsorbent leading to more active adsorption sites and hence more bleaching power. It is important to note that increasing the dose results in a rapid improvement in efficiency, but that the improvement in bleaching efficiency tends to level out at a certain point. Increasing the amount of adsorbent used in the groundnut oil bleaching process is crucial for optimizing production.

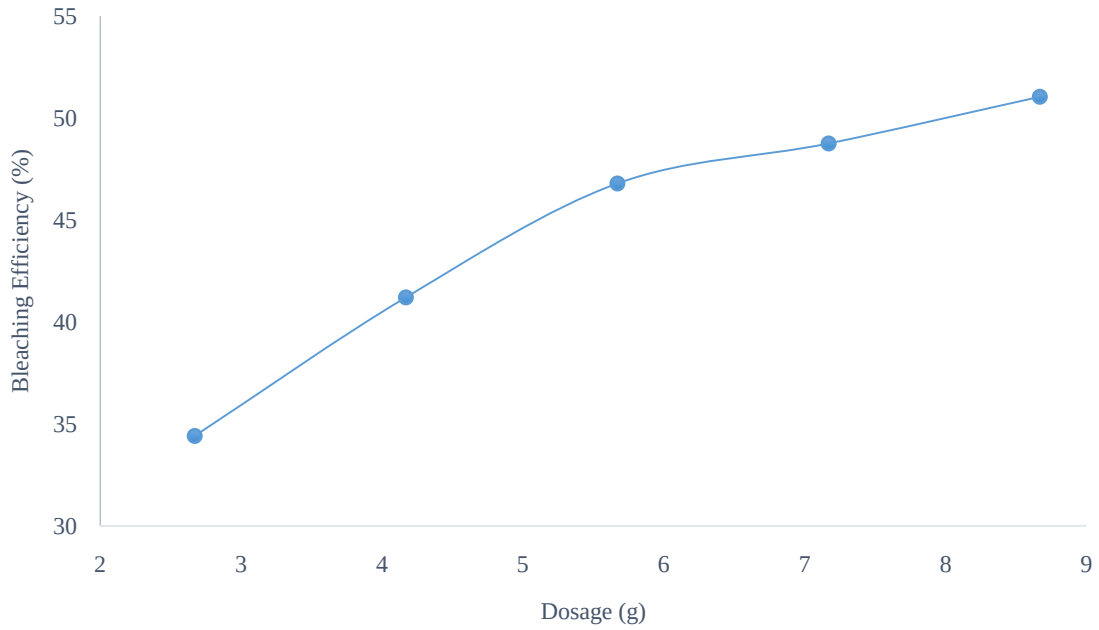

Figure 9: Plot of bleaching efficiency against adsorbent dosage

3.3.2 EFFECT OF TEMPERATURE ON THE BLEACHING PROCESS

Table 3: Absorbance and bleaching efficiency at varying temperatures

Temperature (℃)	Absorbance (A450)	Bleaching Efficiency (%)
34	0.621	35.45
54	0.512	46.78
74	0.502	47.81
94	0.537	44.18

To study this effect, adsorption was performed at different temperature within the range of 34 – 94 ℃ at constant optimum adsorbent dosage, time and particle size (5.67 g, 22 min and 0.2 mm respectively). The absorbance of the crude groundnut oil was measured as 0.962. Figure 4.28 shows that with increased temperature, the bleaching efficiency initially increases until a certain point at which it then begins to decrease. It can be inferred that the bleaching temperature has a direct effect on the bleaching process and the increase in bleaching power occurs as a result of higher energy and adsorption sites provided by the temperature increase and the decrease in bleaching power may be as a result of a destruction of these adsorption sites due to the higher temperatures. Bleaching temperature is an essential aspect of the bleaching of groundnut oil as its rise enhances the effectiveness of the process till a certain point.

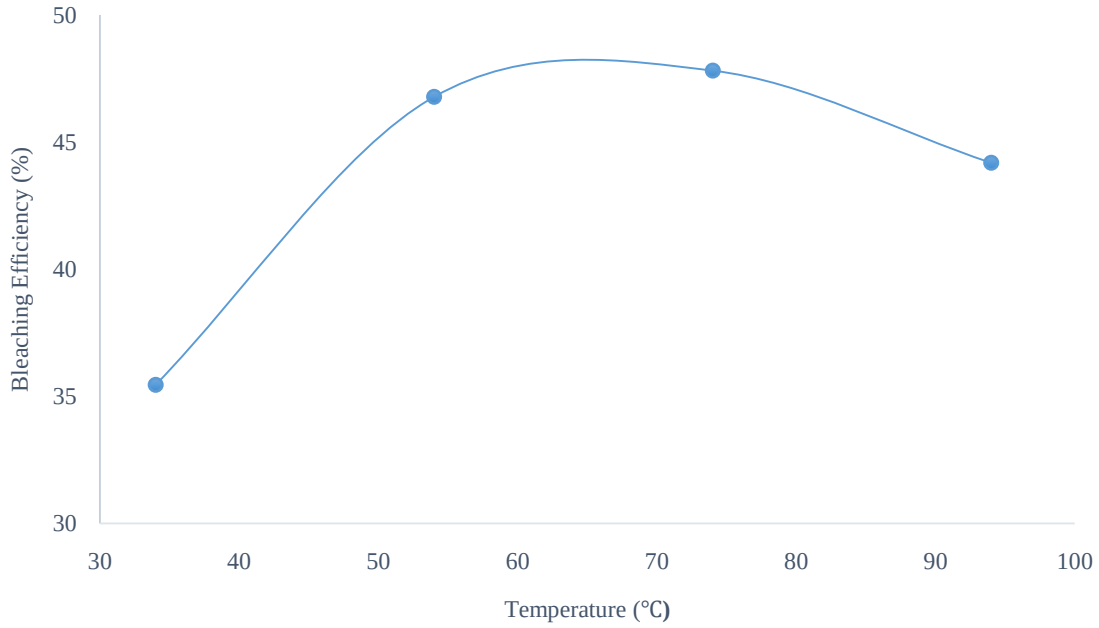

Figure 10: Plot of bleaching efficiency against temperature

3.3.3 EFFECT OF CONTACT TIME ON THE BLEACHING PROCESS

Table 4: Absorbance and bleaching efficiency at varying contact time

Contact Time (min)	Absorbance (A450)	Bleaching Efficiency (%)
12	0.667	30.67
22	0.512	46.78

32	0.485	49.58
42	0.472	50.94
52	0.468	51.35

To study this effect, adsorption was performed at different contact time within the range of 12 – 52 min at constant optimum temperature, adsorbent dosage and particle size (54 ℃, 5.67 g and 0.2 mm respectively). The absorbance of the crude groundnut oil was measured as 0.962. Figure 11 shows that the percentage bleached increased with increase in contact time. It can be inferred that the contact time has a direct effect on the bleaching process and the increase in bleaching power occurs as a result of an increase inadsorption of the adsorbates to the active adsorption sites due to the longer time of contact between them. It should be noted that an initial increase in the contact time leads to a steep increase in the efficiency and further increase in the time tends to plateau the bleaching efficiency increase. Contact time is an important factor of the bleaching of groundnut oil as its increase improves the efficiency of the process.

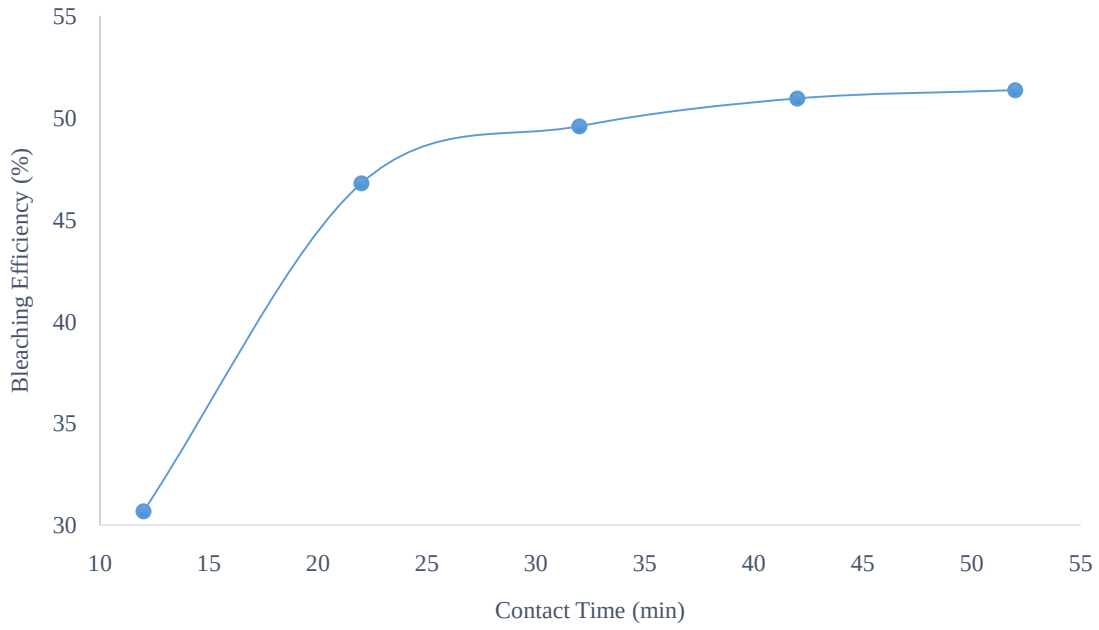

Figure 11: Plot of bleaching efficiency against contact time

3.4 KINETIC STUDIES

The solute absorption rate of a process may be determined by studying its sorption kinetics. It is a crucial factor in determining the success of an adsorption process[14].Table 5 displays the kinetic parameters calculated from the linear plots of the corresponding kinetic equations. In a head-to-head comparison of the analysed data, the pseudo-second-order model (R^2 = 0.9957) was shown to better characterize the adsorption under the optimal circumstances.

Table 5: Kinetic parameters for the adsorption bleaching process

Kinetic Model	**Constants/ Parameters**		
	K_1 (min^{-1})	q_e($mg.g^{-1}$)	R^2
Pseudo-First Order	0.0112	0.3034	0.6532
	K_2 ($g.mg^{-1}.min^{-1}$)	q_e($mg.g^{-1}$)	R^2
Pseudo-Second Order	1.2013	0.4557	0.9957
	K_d($g.mg^{-1}.min^{-1}$)	ε ($mg.l^{-1}$)	R^2
Intra-Particle Diffusion	0.0724	0.9262	0.9357
	$\alpha \times 10^{-5}$ ($mg.g^{-1}.min^{-1}$)	β ($mg.g^{-1}$)	R^2
Elovich	9.5008	7.4906	0.8566

3.4.1 PSEUDO-FIRST ORDER KINETIC MODEL

The linearized Pseudo-first order rate expression is given as:

$$\ln(q_e - q_t) = \ln q_e - K_1 t \qquad (13)$$

Where q_e and q_t are the amounts of adsorbates at equilibrium time and at and time t respectively (mg/g), K_1 is the Pseudo-first order adsorption rate constant (min^{-1}), and t is the contact time (min).

Beer lambert's law gives a direct relation between concentration and absorbance, so the equation can be written in terms of absorbance instead of concentration as follows

$$\ln(A_0 - A_t) = \ln A_0 - K_1 t \qquad (14)$$

Where: $A_t$is the absorbance of the oil bleached at a time t and A_0 is the absorbance of crude or unbleached oil.

The Pseudo-first order at the optimal temperature was expressed by a plot of In (A_0 - A_t) vs t, as shown in the figure below; A_0 and K_1 were calculated from the slope and the intercept,

respectively. It was found that the value of the correlation coefficient (R^2) was 0.6532. It was discovered that the theoretical q_e did not match up well with the experimental q_e. Adsorption is stated to be regarded not to have obeyed the kinetic model, even if the correlation coefficient R^2 is rather high, if the estimated values of q_e are not very near to the observed value of q_e[15].

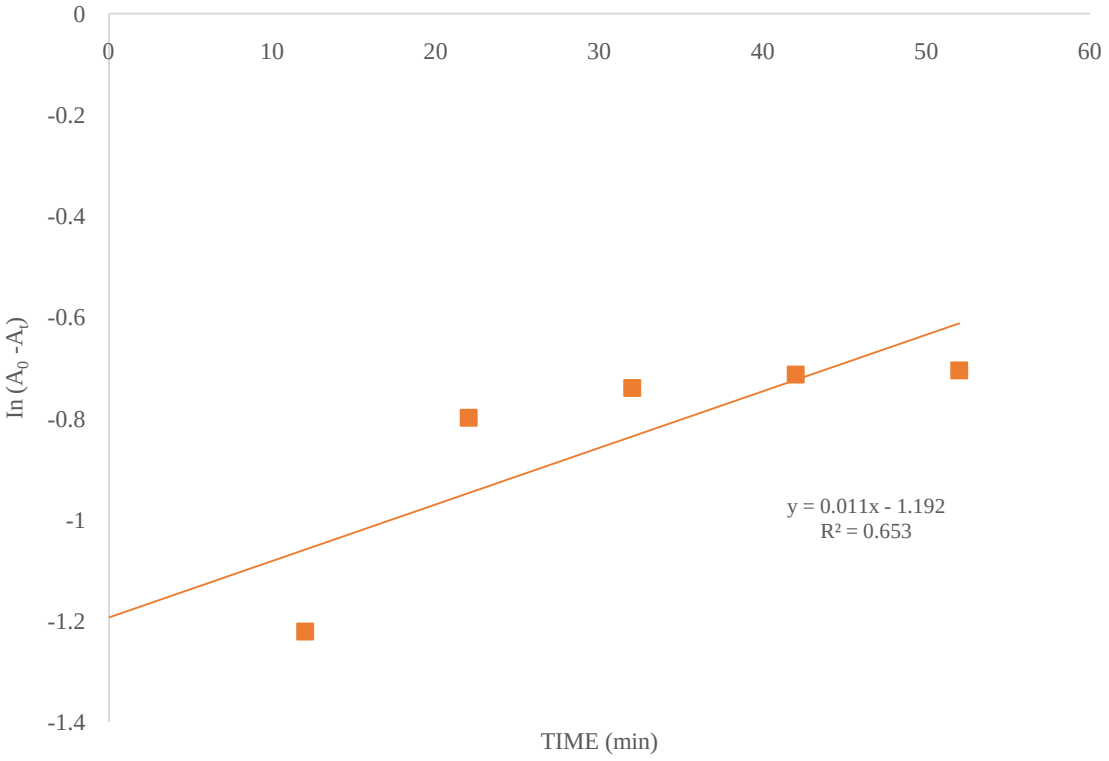

Figure 12: Pseudo-first order kinetic model plot

3.4.2 PSEUDO-SECOND ORDER KINETIC MODEL

The linear form of the pseudo-second orderexpression is:

$$\frac{t}{q_t} = \frac{1}{K_2 q_e^2} + t\left(\frac{1}{q_e}\right) \qquad (15)$$

Where q_e and q_t are the amounts adsorbed atequilibrium time and at any time t respectively(mg/g), K_2 is the Pseudo-second orderadsorption rate constant (g/mgmin), and t is thecontact time (min).

Beer lambert's law gives a direct relation between concentration and absorbance, so the equation can be written in terms of absorbance instead of concentration as follows

$$\frac{t}{A_t} = \frac{1}{K_2 A_e^2} + t\left(\frac{1}{A_t}\right) \qquad (16)$$

Where: $A_t$is the absorbance of the oil bleached at a time t

The slope and intercept of the plot of t/A_t vs t in Fig below were used to calculate the Pseudo-second order rate constant K_2, and A^t for the adsorbent at the optimal temperature.

The adsorbent has an extremely high value of R^2 (0.9957 to be exact). This indicates that the adsorbent is highly correlated with the bleaching process. Equally impressive was the closeness between the estimated and actual values of the equilibrium adsorption capacity (q_e). Since these adsorbents are effective in bleaching palm oil, the Pseudo-second-order model may be reliablyapplied to this process.

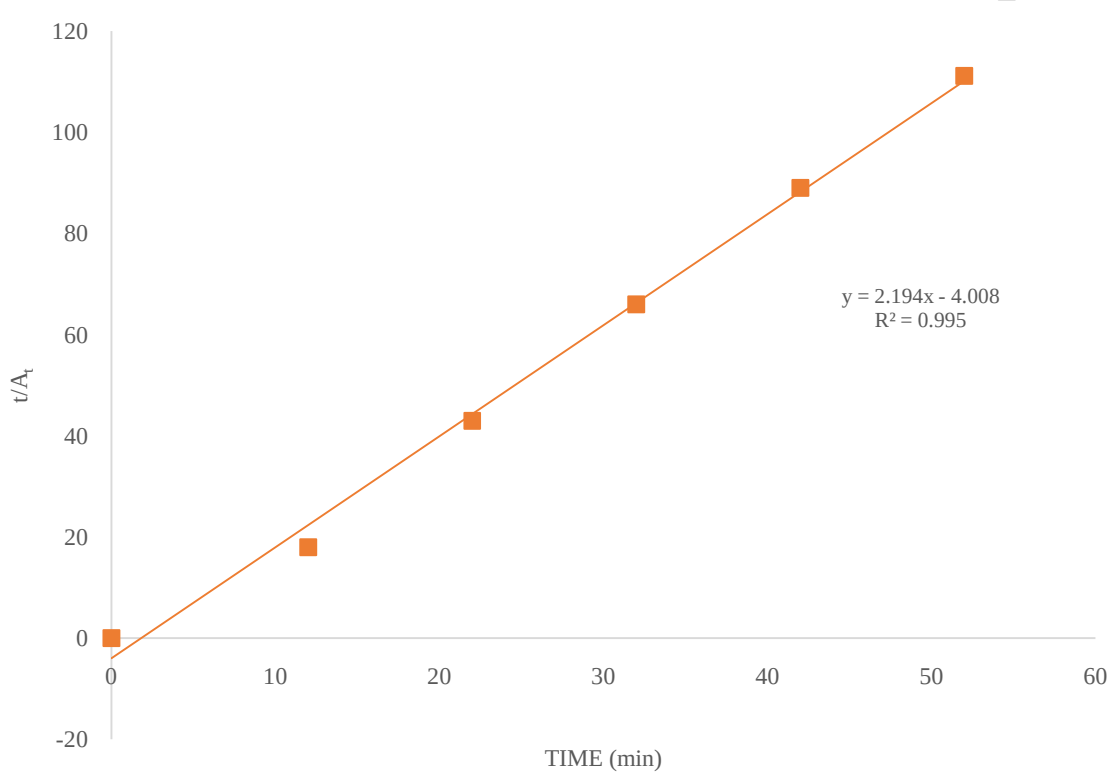

Figure 13: Pseudo-second order kinetic model plot

3.4.3 INTRA-PARTICLE DIFFUSION KINETIC MODEL

The most commonly used technique for identifying the mechanism involved in the adsorption process is the intra-particle diffusion plot which expresses the relationship between the adsorption capacity (q_t) at time $t^{1/2}$. The intra-particle diffusion equation is as expressed below:

$$q_t = K_d t^{0.5} + \varepsilon \quad (17)$$

Where q_t is the amount adsorbed at time t (mg/g), K_d is the rate constant of the intra particle transport (g/mg/min), ε is the equilibrium concentration associated with boundary layer thickness (mg/l), and t is the contact time (min).

Beer lambert's law gives a direct relation between concentration and absorbance, so the equation can be written in terms of absorbance instead of concentration as follows

$$A_t = K_d t^{0.5} + \varepsilon \quad (18)$$

Where: $A_t$is the absorbance of the oil bleached at a time t.

The slope and intercept of the A_t against $t^{0.5}$ plot were used to calculate the intra-particle diffusion rate constants, K_d and ε, for the adsorbent at the optimal temperature. Intra-particle diffusion is the only rate-limiting mechanism if the linear plot of A_t against $t^{1/2}$ is a straight line from the origin [16]. In a batch process, the adsorption of a thin layer of solute onto a solid surface from the entire volume of the solution is the rate limiting step[17]. Due to the change in the rate of mass transfer from the first to the last stage of adsorption, the linear lines did not intersect at the origin. This suggests that intra-particle transport is not the only rate-limiting process, as seen by the linear lines' departure from the origin. Although, the calculated correlation coefficient R^2 was relatively high at a value of 0.9357.

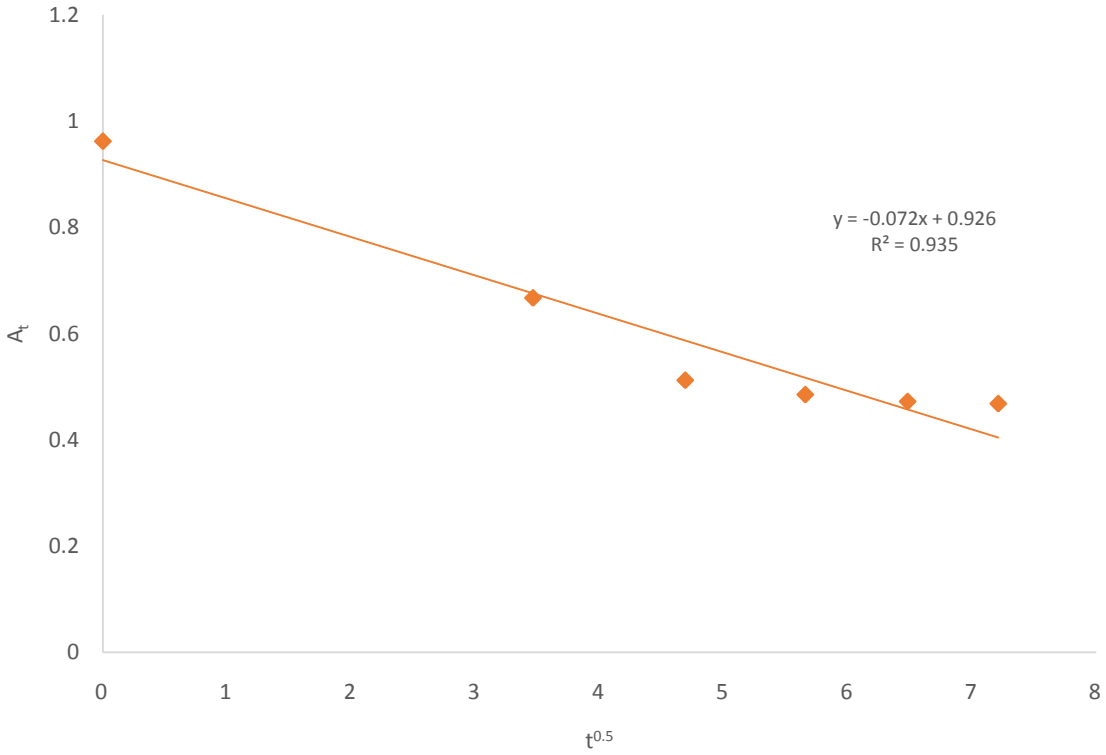

Figure 14: Intra-particle diffusion kinetic model plot

3.4.4 ELOVICH KINETIC MODEL

The linear form of the Elovich kinetic model is expressed below:

$$q_t = (1/\beta)\ln(\alpha\beta) + (1/\beta)\ln(t) \quad (19)$$

Where, α is the parameter of the Elovich model associated with the initial velocity ($mg.g^{-1}min^{-1}$) and β is the desorption constant ($mg.g^{-1}$).

Beer lambert's law gives a direct relation between concentration and absorbance, so the equation can be written in terms of absorbance instead of concentration as follows

$$A_t = (1/\beta)\ln(\alpha\beta) + (1/\beta)\ln(t) \qquad (20)$$

Where: $A_t$is the absorbance of the oil bleached at a time t.

The Elovich model rate constants, α and β for the adsorbent at optimum temperature were determined from the slope and intercept of the plot of A_t against In (t). The calculated correlation coefficient of R^2 was found to be 0.8566.

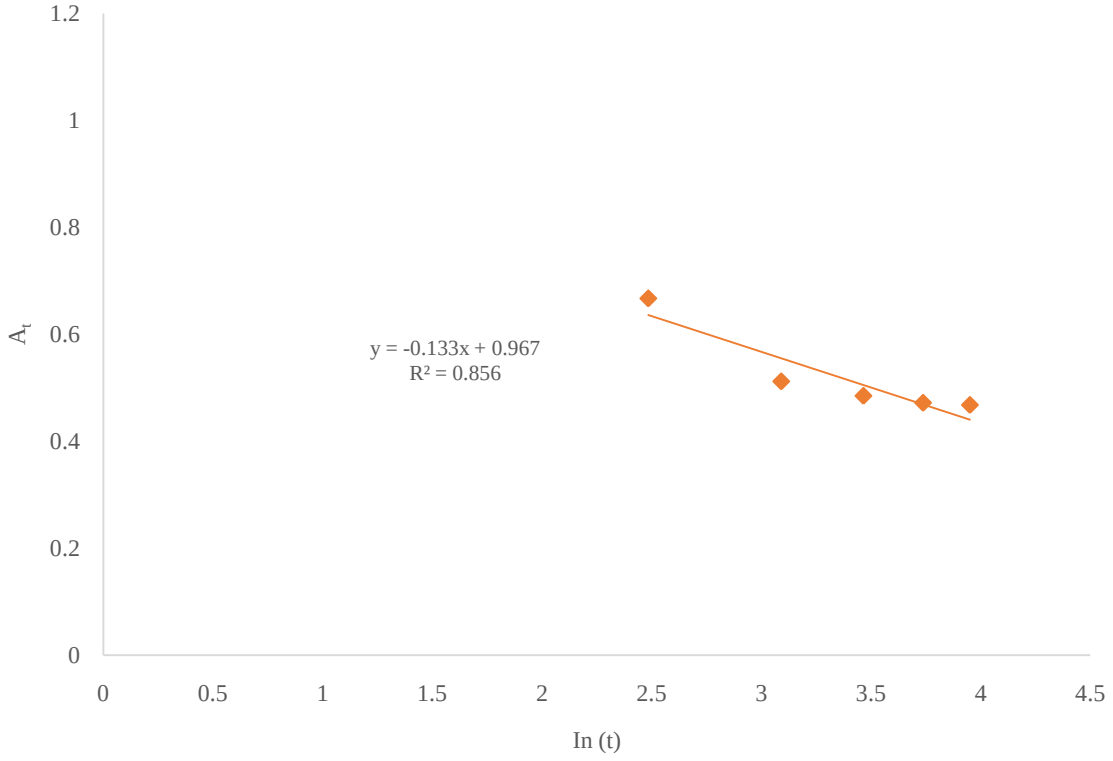

Figure 15: Elovich kinetic model plot

3.5 EQUILIBRIUM AND ISOTHERM STUDIES

The adsorption isotherm describes the connection between the concentration of the solute in the liquid phase and the quantity of adsorbent mass needed to remove the solute, held constant throughout time and temperature. In order to construct an effective adsorption system, one must first get the adsorption isotherm[18]. Adsorption capacity of activated rice husk for bleaching crude groundnut oil was calculated using many adsorption isotherm models for optimal understanding of the adsorption process. The Temkin isotherm was shown to be more favourable to the adsorption process than the other isotherms by comparing their correlation coefficient (R^2) values after the linearization and charting of the linear straight-line connections. This shown that temperature is very influential in the energy required for sorption processes. Certain energy parameters were revealed via the Temkin and Dubinin-Radushkevich constants. Because the

Dubinin-Radushlkevich Isotherm's deviations are not predicated on ideal assumptions like eqi-potential of sorption sites, lack of steric hindrances between sorbed and incoming particles, and surface homogeneity on the microscopic level, it is the most universal of the isotherms. Table 6 below shows the isotherm parameters for the considered isotherms at the various temperatures they were studied.

Table 6: Adsorption isotherm parameters for the bleaching process

Isotherm Model	**Parameter/ Constant**	**Temperature (℃)**			
		34	54	74	94
Freundlich	K_F	0.1670	0.4379	0.8638	0.7291
	1/n	2.3298	2.6550	3.5196	3.6108
	R^2	0.9292	0.9721	0.9287	0.9849
Langmuir	K_L	0.8717	1.1397	1.3438	1.3073
	q_m	0.0461	0.0519	0.0359	0.0318
	R^2	0.7607	0.8713	0.7945	0.9770
Temkin	$b_T \times 10^3$	7.6599	5.1024	3.8480	4.2475
	A_T	2.3726	2.7168	2.5418	2.4134
	R^2	0.9532	0.9948	0.9737	0.9508
Dubinin-Radushlkevich	$B_D \times 10^{-4}$	7.5677	7.5691	9.3988	9.1413
	q_D	2.2516	6.4165	29.2820	27.4600
	E_D	25.7041	25.7018	23.0648	23.3874
	R^2	0.9317	0.9762	0.9347	0.9832

3.5.1 FREUNDLICH ISOTHERM

A linear form of the Freundlich Isotherm expression:

$$\ln q_e = \ln K_f + \frac{1}{n} \ln C_e \quad (21)$$

Where q_e is the number of adsorbates at equilibrium time (mg/g), K_f is the Freundlich equilibrium constant which signifies adsorptive capacity (mg/g), and C_e represents the equilibrium concentration of mixture ($mg.L^{-1}$)

The adsorption process of pigments and oxidation products was tracked using absorbance values according to the Lambert-Beer Law, which states that absorbance values are directly proportional to the concentration of the molecule in the solution.

Thus,

$$C \propto Abs_t = X_e,\ q \propto (Abs_0 - Abs_t)/m = x/m \quad (22)$$

where Abs_0 is the initial absorbance of the solution (before adsorption), Abs_t is the absorbance of the solution in equilibrium after adsorption, and m is the amount of adsorbent used (g). Therefore, the isotherms q vs C were replaced by the following relationship:

x/m vs X_e

Therefore, the Freundlich isotherm becomes:

$$\text{Log } x/m = \log K_f + \frac{1}{n} \log X_e \quad (23)$$

Where x/m is the amount of adsorbate per unit mass of adsorbent (mg/g), X_e is the solute equilibrium concentration of adsorbate (mg/l). Therefore, the Freundlich isotherm was studied by plotting log x/m versus log X_e, as seen in the figure below. Both the intercept and the slope were used to get the Freundlich constants K_f and $\frac{1}{n}$. Adsorption capacity is quantified by the constant K_f, whereas adsorption strength or favourability is quantified by the constant $\frac{1}{n}$. The value of $\frac{1}{n}$ will be between zero and ten for favourable adsorption [19].In this study, the activated rice husk was shown to have a positive effect on the crude groundnut oil, with $\frac{1}{n}$ values ranging from 2.3298 to 3.6108. Adsorption fit the Freundlich isotherm model, as shown by the R^2 values between 0.9287 and 0.9849. The K_f value represents the ability of the adsorbent to remove colour from any given solute. K_f values rose with increasing temperature, showing an increase in the availability of adsorption sites, but fell marginally at the maximum temperature of 94 °C, suggesting that even this high heat might be damaging to the adsorption sites.

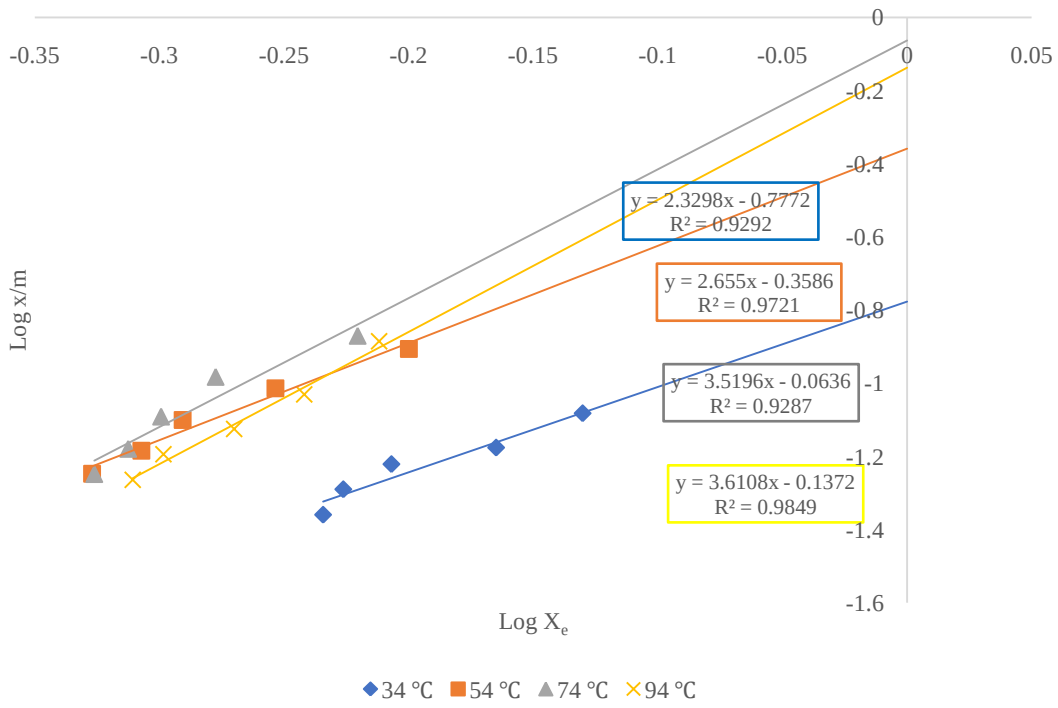

Figure 16: Freundlich isotherm plot for the bleaching process at different temperatures

3.5.2 LANGMUIR ISOTHERM

A linear form of the Langmuir Isotherm expression:

$$\frac{1}{q_e} = \frac{1}{q_m} + \frac{1}{q_m K_L C_e} (24)$$

Where K_L is the Freundlich equilibrium constant which signifies adsorptive capacity (mg/g) and q_m is the theoretical isotherm saturation capacity ($mg.g^{-1}$)

Therefore, the Langmuir isotherm becomes:

$$\frac{X_e}{x/m} = \frac{1}{q_m K_L} + \frac{1}{q_m} X_e (25)$$

The Langmuir constants K_L and q_m were calculated by determining the intercept and the slope of the linear plot of $X_e/(x/m)$ vs X_e in the figure below. R^2 values for the treated Rice husk varied from 0.7607 to 0.9770. This demonstrates that the adsorption is a close fit to the Langmuir isotherm. It's possible that the uniform arrangement of active sites on the activated rice husk is responsible for the good match between the Langmuir isotherm and the experimental results.

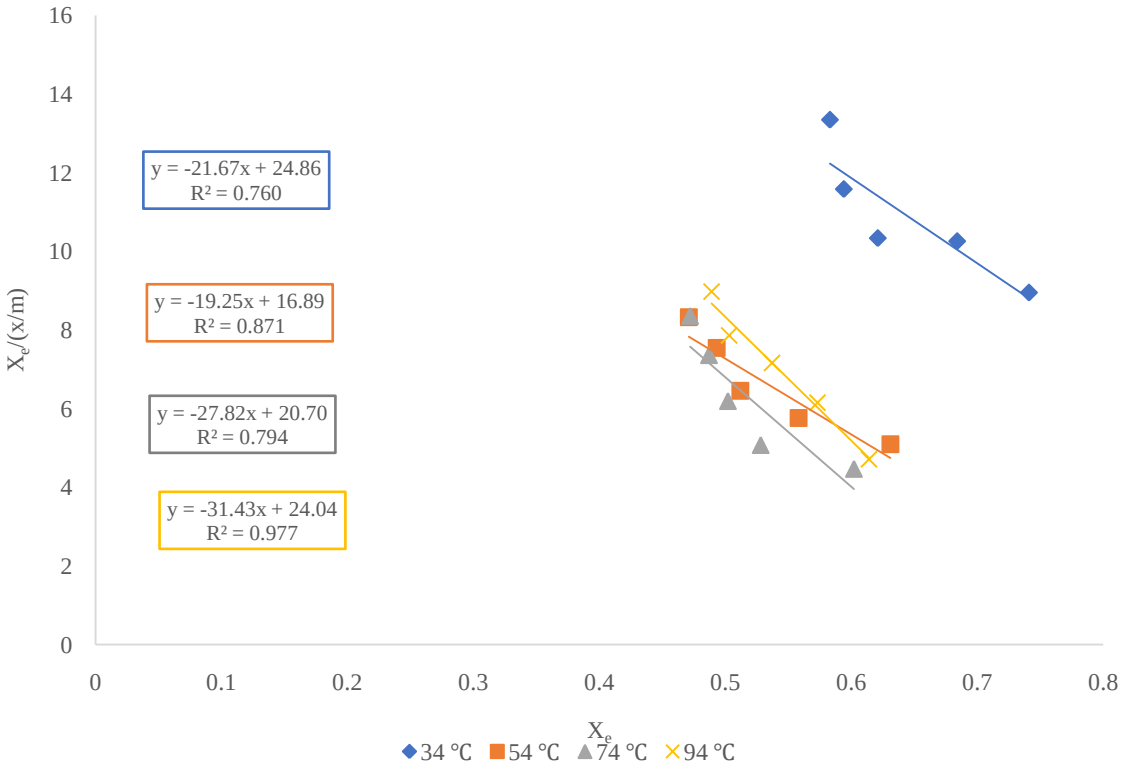

Figure 17: Langmuir isotherm plot for the bleaching process at different temperatures

3.5.3 TEMKIN ISOTHERM

A linear form of the Temkin Isotherm expression:

$$q_e = \frac{RT}{b_T} \ln A_T + \frac{RT}{b_T} \ln C_e \quad (26)$$

Where A_T is the Temkin isotherm equilibrium binding constant ($L.mol^{-1}$),b_T is the Temkin isotherm constant (J/mol), R is the Universal Gas Constant ($J.mol^{-1}.K^{-1}$) and T is the absolute temperature (K)

Therefore, the Temkin isotherm becomes:

$$\frac{x}{m} = \frac{RT}{b_T} \log A_T + \frac{RT}{b_T} \log X_e \quad (27)$$

For the Temkin isotherm, the values of x/m were plotted against Log X_e in the figure below and the Temkin constants A_T and b_T were obtained from the intercept and slope of the plot.

The Temkin model is often used to illustrate surface energy systems with a heterogeneous composition. Temkin isotherm equilibrium binding constant and heat of sorption are denoted by the constants AT and b_T, respectively. Adsorption was shown to be represented by a linear connection in the plot.

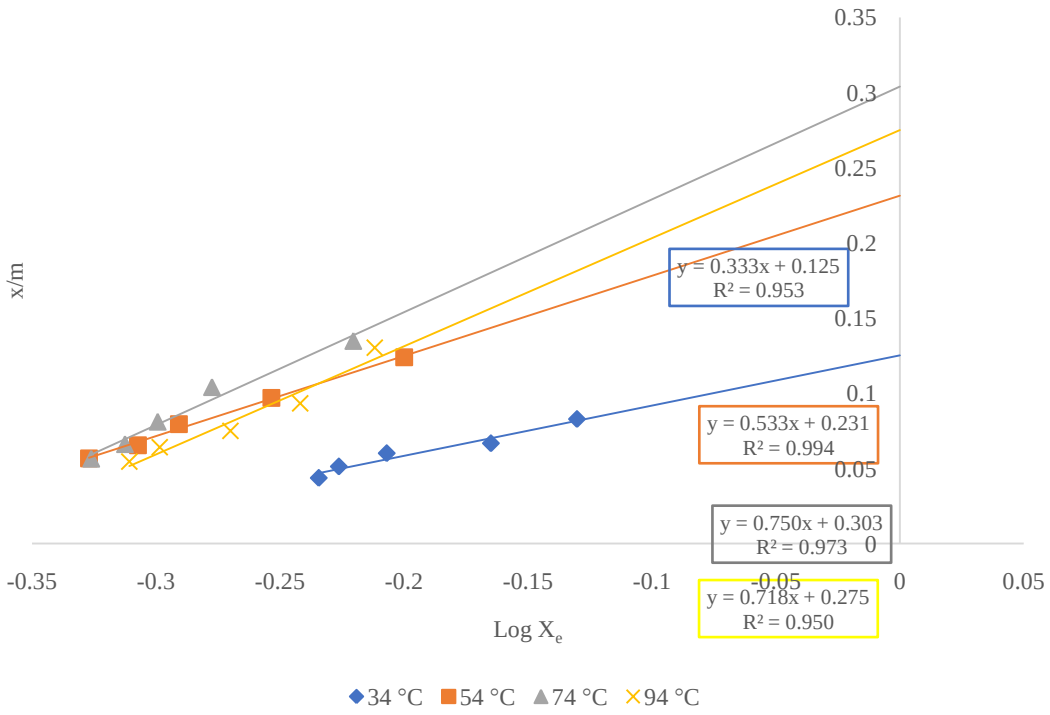

Figure 18: Temkin isotherm plot for the bleaching process at different temperatures

3.5.4 DUBININ-RADUSHKEVICH ISOTHERM

A linear form of the Dubinin-RadushkevichIsotherm expression:

$$\ln q_e = \ln q_D - 2B_D RT \ln(1 + 1/C_e) \quad (28)$$

$$E_D = \sqrt{1/2B_D} \quad (29)$$

Where B_D relates to the free energy of adsorption per mole of coloured oil pigment in the solution as it moves to the surface of the adsorbent from an infinite distance ($mol^2.kJ^2$), q_D is the Dubinin–Radushkevich isotherm constant, which relates to the degree of sorbate sorption on the sorbent surface ($mg.g^{-1}$), E_D is the apparent energy of adsorption ($kJ.mol^{-2}$). The adsorption process of pigments and oxidation products was tracked using absorbance values according to the Lambert-Beer Law, which states that absorbance values are directly proportional to the concentration of the molecule in the solution.

Therefore, the Dubinin-Radushkevich isotherm becomes:

$$\ln \frac{x}{m} = \ln q_D - 2B_D RT \ln(1 + 1/X_e) \quad (30)$$

For the Dubinin-Radushkevich isotherm, the values of Log x/m were plotted against Log $(1 + 1/X_e)$ in the figure below. Using the graph's intercept and slope, we can get the constants B_D and q_D. Apparent energy of heterogeneous surface systems is the primary application of the concept. The plot's linearity also revealed the sort of adsorption relationship present on the adsorbents. Chemisorption was detected by an E_D value greater than 8 $kJ.mol^{-1}$.

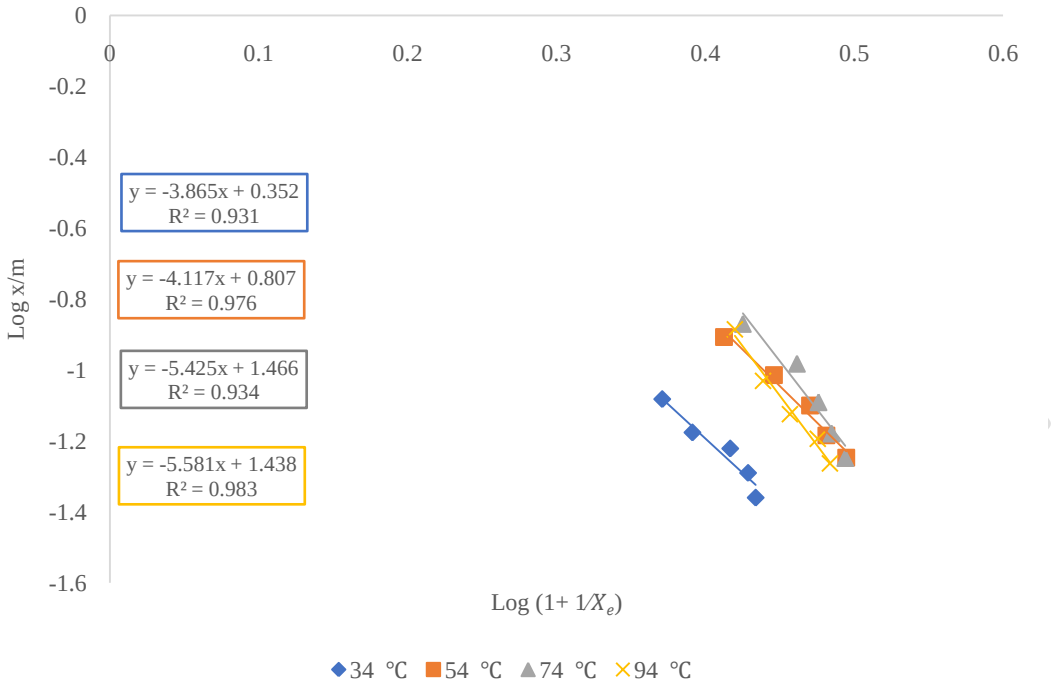

Figure 19: Dubinin-Radushkevich isotherm plot for the bleaching process at different temperatures

3.6 THERMODYNAMIC STUDIES

Changes in free energy (ΔG^0_{ads}), enthalpy (ΔH^0_{ads}), and entropy (ΔS^0_{ads}) were used to assess thermodynamic attributes. An increase or reduction in the unpredictability of the process at the solid/solution interface is determined by ΔS^0_{ads}, whereas ΔG^0_{ads} controls whether or not the process is viable and spontaneous. If ΔG^0_{ads} is negative, then reactions take place spontaneously at a given temperature [20].Sorption distribution coefficient of the isotherm with the best match may be used to quickly and easily calculate the thermodynamic parameters from data acquired from adsorption isotherm models. This situation calls for the use of the Temkin isotherm. The free energy of the sorption process was calculated by plugging the A_T values into the following equation:

$$\Delta G^0_{ads} = -RT \ln A_T \quad (31)$$

Where ΔG^0_{ads} is the free energy of sorption (kJ/mol), T is the temperature in Kelvin and R is the universal gas constant (8.31414 J/mol K). Below is the Van't Hoff equation for the sorption distribution coefficient as a function of temperature in terms of the enthalpy change ΔH^0_{ads} and the entropy change ΔS^0_{ads}:

$$\ln(A_T) = \frac{\Delta S^0_{ads}}{R} - \frac{\Delta H^0_{ads}}{RT} \quad (32)$$

Where ΔH^0_{ads} is the heat of adsorption (kJ/mol) and ΔS^0_{ads} is the standard change in entropy (kJ/mol). A larger negative value for the free energy represents a more energetically

favourablesorption process, which in turn shows the degree to which the sorption process occurs spontaneously. Slope and intercept of a 1/T vs ln A_T scatter plot were used to calculate ΔH^0_{ads} and ΔS^0_{ads}, respectively. (Fig. 20). Table 7 displays the results of the calculations.

Table 7: Thermodynamic parameters for the bleaching process

Temperature (K)	ΔG^0_{ads} (KJ/mol)	ΔH^0_{ads} (KJ/mol)	ΔS^0_{ads}(J/mol)
307	-2.2053	-2.9014	-0.5787
327	-2.7174		
347	-2.6914		
367	-2.6882		

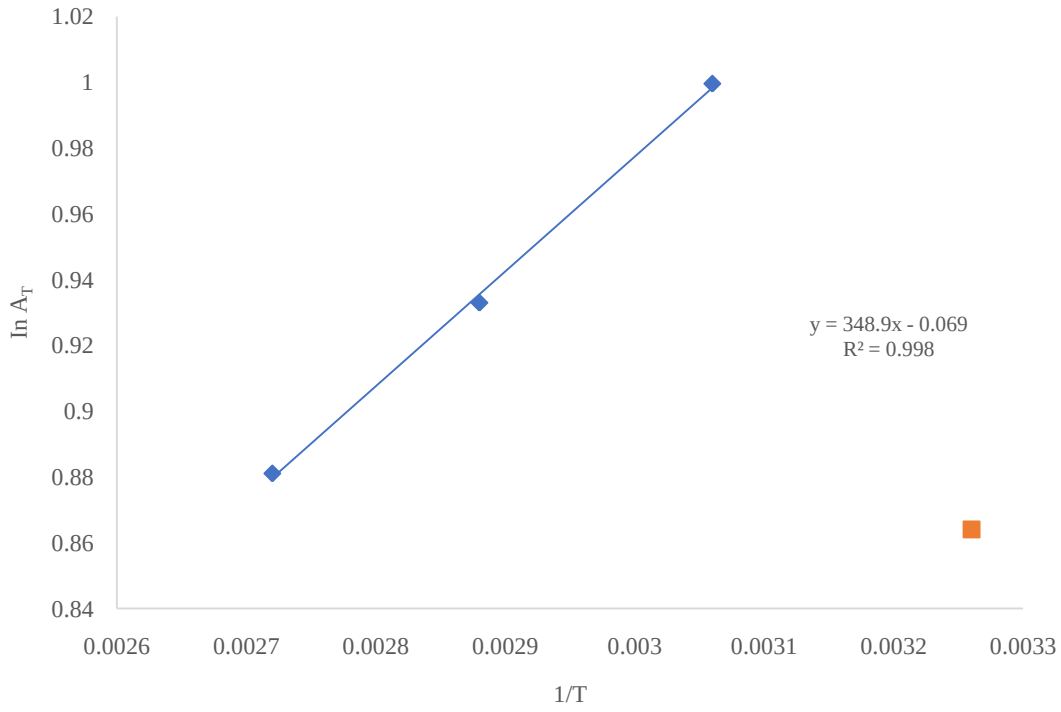

Figure 20: Thermodynamic plot for the bleaching process

As can be seen in Table 7, all ΔG^0_{ads} values are negative, and the degree of negativity grows with rising temperature. Since ΔG^0_{ads} is negative, adsorption bleaching occurs spontaneously and is technically feasible. This demonstrates that greater temperatures facilitate the bleaching process.

It is true that the enthalpy of adsorption, ΔH_{ads}^{0}, and not the entropy of adsorption, ΔG_{ads}^{0}, dictates the type of adsorption, yet values of ΔG_{ads}^{0} in the range of 2.2053-2.7174 kJ/ mol are typical of physical adsorption systems.

Since ΔH_{ads}^{0} is negative, energy is being given off throughout the adsorption process; thus, this is an exothermic reaction. Given that ΔH_{ads}^{0} is less than 20 KJ/mol, adsorption may be classified as a physisorption process. Since disorder is related to entropy, a negative value of ΔS_{ads}^{0} implies less order, i.e., the crude oil has less colorant and fewer contaminants after the bleaching process.

4. CONCLUSION

The kinetic, equilibrium and thermodynamic study of groundnut oil bleaching using adsorbent developed from activated Rice husk been investigated in this work. A BET analysis carried out on the crude and acid activated rice husk showed a surface area increase from 150.32 m^2/g to 1450.32 m^2/g which was further validated by the SEM micrograph images obtained. The adsorption characteristics of the bleaching process showed that adsorbent dosage, bleaching temperature and contact time are all important parameters to be considered during the bleaching process. The kinetic data of the bleaching process were best described by the pseudo-second order kinetic model while the equilibrium adsorption isotherm analysis showed that the results from the Temkin isotherm were the most significant. The thermodynamic study revealed that the adsorptive bleaching process is feasible, spontaneous, exothermic with a decrease in entropy. The enthalpy value also showed that the adsorption process is predominantly physisorption. This study has revealed that an effective adsorbent can be produced from rice husk under optimized process conditions.

REFERENCES

[1] G. Mieth, "Peanuts: Production Processing, Products. 3. Aufl. Herausgegeben von J. G. Woodroof. 414 Seiten, zahlreiche Abb. und Tab. AVI Publishing Company, Inc., Westport, Connecticut, 1983. Preis: 63.50 $," *Food/Nahrung*, vol. 28, no. 8, 1984, doi: 10.1002/food.19840280822.

[2] R. A. Moreau, D. B. Johnston, M. J. Powell, and K. B. Hicks, "A comparison of commercial enzymes for the aqueous enzymatic extraction of corn oil from corn germ," *JAOCS, J. Am. Oil Chem. Soc.*, vol. 81, no. 11, 2004, doi: 10.1007/s11746-004-1023-3.

[3] V. P. Della, I. Kühn, and D. Hotza, "Rice husk ash as an alternate source for active silica production," *Mater. Lett.*, vol. 57, no. 4, 2002, doi: 10.1016/S0167-577X(02)00879-0.

[4] M. R. Gidde and A. P. Jivani, "Waste to Wealth - Potential of Rice Husk in India a Literature Review," *Proc. Int. Conf. Clean. Technol. Environ. Manag.*, 2007.

[5] N. Soltani, A. Bahrami, M. I. Pech-Canul, and L. A. González, "Review on the physicochemical treatments of rice husk for production of advanced materials," *Chemical Engineering Journal*, vol. 264. 2015. doi: 10.1016/j.cej.2014.11.056.

[6] 2014 Shwetha et al, "Shwetha et al,. 2014," *Oppor. Prospect. Manag. Rice Husk*, vol. Volume 7 |, no. 1, pp. 176–180, 2014.

[7] K. R. D and P. P.R.T, “Stabilization of Expansive Soil With Rice Husk Ash, Lime and Gypsum – an Experimental Study,” *Int. J. Eng. Sci. Technol.*, vol. 3, no. 11, 2011.

[8] B. I. UGHEOKE, E. O. ONCHE, O. N. NAMESSAN, and G. A. ASIKPO, “Property Optimization of Kaolin-Rice Husk Insulating Fire-Bricks,” *Leonardo Electron. J. Pract. Technol.*, vol. 9, no. 9, 2006.

[9] A. Mandal, P. Mukhopadhyay, and S. K. Das, “The study of adsorption efficiency of rice husk ash for removal of phenol from wastewater with low initial phenol concentration,” *SN Appl. Sci.*, vol. 1, no. 2, 2019, doi: 10.1007/s42452-019-0203-3.

[10] Z. Hu and M. P. Srinivasan, “Preparation of high-surface-area activated carbons from coconut shell,” *Microporous Mesoporous Mater.*, vol. 27, no. 1, pp. 11–18, Jan. 1999, doi: 10.1016/S1387-1811(98)00183-8.

[11] J. Guo and A. C. Lua, “Textural and chemical properties of adsorbent prepared from palm shell by phosphoric acid activation,” *Mater. Chem. Phys.*, vol. 80, no. 1, 2003, doi: 10.1016/S0254-0584(02)00383-8.

[12] E. Y. L. Teo *et al.*, “High surface area activated carbon from rice husk as a high performance supercapacitor electrode,” *Electrochim. Acta*, vol. 192, pp. 110–119, Feb. 2016, doi: 10.1016/j.electacta.2016.01.140.

[13] V. Gibon, W. De Greyt, and M. Kellens, “Palm oil refining,” *Eur. J. Lipid Sci. Technol.*, vol. 109, no. 2007, pp. 315–335, 2007.

[14] S. Arivoli, M. Hema, and P. M. D. Prasath, “Adsorption of Malachite Green Onto Carbon Prepared From Borassus Bark Adsorption of Malachite Green Onto Carbon Prepared From,” *Arab. J. Sci. Eng.*, vol. 34, no. 2, 2009.

[15] M. J. Iqbal and M. N. Ashiq, “Thermodynamics and kinetics of adsorption of dyes from aqueous media onto alumina,” *J. Chem. Soc. Pakistan*, vol. 32, no. 4, 2010.

[16] Ö. Gök, A. S. Özcan, and A. Özcan, “Adsorption kinetics of naphthalene onto organo-sepiolite from aqueous solutions,” *Desalination*, vol. 220, no. 1–3, 2008, doi: 10.1016/j.desal.2007.01.025.

[17] S. Goswami and U. C. Ghosh, “Studies on adsorption behaviour of Cr(VI) onto synthetic hydrous stannic oxide,” *Water SA*, vol. 31, no. 4, 2005, doi: 10.4314/wsa.v31i4.5150.

[18] R. Rajeshkannan, M. Rajasimman, and N. Rajamohan, “Removal of malachite green from aqueous solution using hydrilla verticillata - optimization, equilibrium and kinetic studies,” *World Acad. Sci. Eng. Technol.*, vol. 37, 2010.

[19] R. S. Raveendra, P. A. Prashanth, B. R. Malini, and B. M. Nagabhushana, “Adsorption of Eriochrome black-T azo Dye from Aqueous solution on Low cost Activated Carbon Prepared from Tridax procumbens,” *Res. J. Chem. Sci.*, vol. 5, no. 3, 2015.

[20] A. Omri, A. Wali, and M. Benzina, “Adsorption of bentazon on activated carbon prepared from Lawsonia inermis wood: Equilibrium, kinetic and thermodynamic studies,” *Arab. J. Chem.*, vol. 9, 2016, doi: 10.1016/j.arabjc.2012.04.047.